Optimization of Handover Parameters for Traffic Sharing in GERAN

Matías Toril (mtoril@ic.uma.es)
*Communications Engineering Dept., University of Málaga**

Volker Wille (volker.wille@nokia.com)
Performance Services, Nokia Siemens Networks

October 16, 2007

Abstract. Cellular network traffic is unevenly distributed both in time and space, which greatly complicates network dimensioning. As a result, some cells in the network are permanently congested, while others are underutilized. In a previous paper, the authors showed that this problem can be effectively solved in GSM/EDGE Radio Access Networks (GERAN) by modifying handover boundaries. However, several drawbacks prevent operators from fully exploiting the potential of this technique. This paper investigates the limitations of current traffic-sharing approaches with tight frequency reuses in GERAN. To deal with such limitations, an algorithm is proposed to jointly optimize handover margins and signal-level constraints based on network statistics for traffic sharing in GERAN. A complementary algorithm is proposed to adjust cell (re)selection offsets to minimize the number of handovers. Simulation results show that the proposed method achieves a significant reduction in call blocking without excessive call quality impairment or increase of network signaling load when compared to the current approaches. More traffic can thus be handled without the need for any hardware upgrades, providing a cost-effective means to increase network capacity.

Keywords: mobile network, optimization, traffic sharing, handover, fuzzy

Abbreviations: ACRO – Adaptation of Cell Reselection Offsets; BCCH – BroadCast CHannel; CIR – Carrier-to-Interference Ratio; CRS – Cell (Re)Selection; DR – Directed Retry; EDGE – Enhanced Data rates for Global Evolution; FER – Frame Erasure Rate; FSHMC – Fuzzy Slow Handover Margin Control; FOSLC – Fuzzy Optimization of Signal-Level Constraints; GERAN – GSM/EDGE Radio Access Network; GSM – Global System for Mobile Communications; HO – HandOver; NMS – Network Management System; OSLC – Optimization of Signal Level Constraints; PBGT – Power BudGeT; RRM – Radio Resource Management; SHMC – Slow Handover Margin Control; TCH – Traffic CHannel; TRHO – Traffic Reason HandOver

1. Introduction

In recent years, the size and complexity of cellular networks has increased exponentially, turning network management into an extremely challenging task. This issue has stimulated intense research in the field of self-tuning networks [1][2][3][4]. The self-tuning property refers to the capability to modify their parameters autonomously based on statistical performance measurements. This capability is crucial for mature technologies, such as GERAN, where an efficient network management is needed to provide high-quality services at a low operational cost.

Traffic management is one of the main areas where self-tuning has been applied in GERAN. Several studies (e.g., [5][6]) have shown that cellular traffic tends to be unevenly distributed both in time and space. Fast fluctuations in traffic demand are dealt with through Radio Resource Management (RRM) procedures, such as dynamic half-rate coding [7], directed retry [8] and dynamic load sharing [9][10][11]. While the former relieves congestion in a cell by temporarily increasing the number of traffic channels, the latter

* This work was supported by TIC2003-07827 grant from the Spanish Ministry of Science and Technology.

take advantage of overlapping between neighbor cells to divert calls to cells in which spare capacity is available. These reactive mechanisms, conceived to deal with the randomness of the call process, are unable to solve localized congestion problems caused by uneven spatial traffic distribution. As many dynamic processes, these mechanisms are prone to instability, which forces the use of conservative internal settings. For this reason, localized congestion problems are counteracted in the long term by planning strategies, such as the extension of transceivers or cell splitting. In the short term, the adaptation of cell service areas remains the only solution for those cells that cannot be upgraded quickly or simply do not justify the deployment of additional resources. The latter case can be the situation where congestion is due to seasonal traffic only.

Several techniques have been proposed to adjust the service area of a cell in GERAN. A first group modifies physical parameters in the base station, such as transmitted power [12] or antenna radiation pattern [13]. As these actions affect coverage and may require visiting the site, they are seldom used. Alternatively, a second group modifies parameters in RRM processes, such as Cell (Re)Selection (CRS) and HandOver (HO) [14]. As tuning CRS parameters is only effective during call set-up, the optimization of HO parameters, such as the HO margins, is the preferred option. To tune HO margins, proactive approaches formulate the tuning problem as a classical optimization problem, which can be solved exactly [15][16]. Unfortunately, the required analysis tool is rarely available for cost reasons. Therefore, operators have to solve the problem by heuristic methods. Field trial results presented in [17] showed that adapting the diffusive load sharing algorithm in [10][11] for its use in the Network Management System (NMS) can increase network capacity with existing resources. However, to the authors' knowledge, no comprehensive analysis of the limits of this technique has been published. Likewise, no thorough comparison against other congestion-relief techniques has been performed.

This paper investigates traffic sharing for voice services in GERAN in an extreme, albeit realistic, scenario. The limitations of classical approaches under severe congestion and tight frequency reuses are put into evidence. To circumvent these limitations, a novel heuristic method is proposed to tune several parameters in a standardized HO algorithm based on statistics in the NMS. The method equalizes network congestion, while avoiding call quality problems, by jointly optimizing HO margins and signal-level constraints on a per-adjacency basis. For this purpose, the method combines two algorithms already presented in [17] and [18], which have been used separately in the past. It will be shown here that the combination of both algorithms extends the limits of the individual approaches. As main novelty, these algorithms adapt internal parameters to the current state of margins in the adjacency. In addition, a novel method is proposed to adjust CRS offsets on a per-cell basis to synchronize cell service areas in CRS and HO. Thus, the number of unnecessary HOs is minimized. Performance assessment is based on system-level simulations. During the tests, the proposed method is compared to classical congestion-relief approaches. The rest of the paper is organized as follows. Section 2 describes the HO and CRS algorithms considered, identifying their main parameters and how these are currently set by operators. Section 3 outlines the proposed self-tuning algorithms. Section 4 discusses the simulation results and Section 5 presents the main conclusions of the study.

2. Description of Optimized Parameters

This section describes the main RRM parameters that have an influence on cell service area in GERAN: HO margins, HO signal-level constraints and CRS offsets. For clarity, the HO and CRS processes are treated independently.

2.1. Handover Parameters

In GERAN, Power BudGeT (PBGT) HO ensures that, under normal conditions, any mobile station with a voice connection is served by the base station that provides minimum pathloss [19]. A HO is initiated whenever the average signal level from a neighbor cell exceeds the one received from the serving cell by a certain margin, provided a certain minimum signal level is ensured. These conditions can be formulated as

$$\overline{\mathrm{RXLEV\_NCELL}}_j \geq RxLevMinCell_{i \to j} \,, \tag{1}$$

$$\mathrm{PBGT}_{i \to j} = \overline{\mathrm{RXLEV\_NCELL}}_j - \overline{\mathrm{RXLEV\_DL}} \geq HoMarginPBGT_{i \to j} \,, \tag{2}$$

where $\overline{\mathrm{RXLEV\_NCELL}}_j$ and $\overline{\mathrm{RXLEV\_DL}}$ are the average received signal levels from neighbor cell j and serving cell i, $\mathrm{PBGT}_{i \to j}$ is the power budget of neighbor cell j with respect to serving cell i, and $RxLevMinCell_{i \to j}$ and $HoMarginPBGT_{i \to j}$ are parameters defining the HO signal-level constraint and margin in the adjacency, respectively. Signal-level constraints are used to discard neighbor cells that do not provide good radio signal properties, while margins provide a hysteresis region to ensure HO stability. In this work, signal-level units are dBm and margin units are dB.

In the current approach, operators set HO margins to safe values that are deployed network wide. Subsequent modification of this parameter on a local basis enables operators to re-shape the service area of cells to cope with traffic hotspots. Unfortunately, the gain from tuning margins comes at the expense of reduced call quality and increased interference level throughout the system, since calls are carried in cells other than their nominal (i.e., optimal in terms of radio conditions) cells. To restrict these undesirable effects, only positive margin values are permitted, since the PBGT equation thus ensures that any HO always takes place to a cell offering better signal level. As a consequence, the benefit of optimizing these parameters is not fully exploited.

For HO signal-level constraints, values slightly above receiver sensitivity are normally set to avoid unnecessary discard of candidate cells. This strategy results in a large number of candidate cells, which increases macro-diversity gain from HO in severe shadowing conditions. However, these settings allow HO to a cell that does not provide enough quality. Nonetheless, these loose settings give acceptable results when combined with positive margins, since the latter ensures that only HO to a better cell is permitted. Obviously, this is not the case when margins are adjusted to negative values by the tuning process.

2.2. Cell (Re)Selection Parameters

An idle terminal selects the cell where a call will be initiated based on C1 and C2 criteria [20]. The C1 value is calculated on a per-cell basis as

$$\mathrm{C1}_i = \mathrm{RLA\_C}_i - RxLevAccessMin_i \,, \tag{3}$$

where RLA_C$_i$ is the average received signal level from cell i and $RxLevAccessMin_i$ is a parameter defining the minimum signal level to have access to the network through cell i. Alternatively, the C2 value is calculated as

$$C2_i = \begin{cases} C1_i + CellReselectOffset_i - TemporaryOffset_i \cdot H(PT_i - t) & \text{if } PT_i < 640\text{s}, \\ C1_i - CellReselectOffset_i & \text{if } PT_i = 640\text{s}, \end{cases} \quad (4)$$

where $CellReselectOffset_i$ is a non-negative biasing term for cell i, $TemporaryOffset_i$ is a non-negative number subtracted during the period PT_i, and H(x)=1 if x> 0, 0 otherwise. Thus, the *CellReselectOffset* parameter, which is normally set to 0, can be used to control the dominance area of cells during CRS. In this work, only negative biasing is implemented, as positive biasing might cause that calls are initiated in cells that do not provide adequate signal level. For this purpose, the second line in (4) is used. With this expression, the larger *CellReselectOffset*, the smaller C2, and hence the smaller the dominance area during CRS.

3. Description of Self-Tuning Algorithms

This section outlines several tuning algorithms for the above-described parameters. A first algorithm tunes HO margins for traffic sharing between neighbor cells. A second algorithm tunes HO signal-level constraints to adapt to uneven interference levels in the network. A third algorithm jointly tunes margins and signal-level constraints to make the most of the former algorithms. The last algorithm modifies CRS offsets to synchronize cell service areas in CRS to the ones defined by HO. It is worth noting that all the proposed algorithms are based on statistical information that is currently only available in the NMS. Hence, these algorithms are designed as network re-planning procedures that should be launched periodically (e.g., on a daily basis).

3.1. Tuning of Handover Margins

The diffusive algorithm in [17] balances the blocking rate between adjacent cells by iteratively changing HO margins on each adjacency. The basic balancing rule is

$$\delta HoMarginPBGT_{i\to j}^{(n+1)} = -\beta^{(n)} \cdot \left[BR_i^{(n)} - BR_j^{(n)} \right], \quad (5)$$

$$HoMarginPBGT_{i\to j}^{(n+1)} = HoMarginPBGT_{i\to j}^{(n)} + \delta HoMarginPBGT_{i\to j}^{(n+1)}, \quad (6)$$

where superscripts $^{(n)}$ and $^{(n+1)}$ denote the old and new iteration, $HoMarginPBGT_{i\to j}$ and $\delta HoMarginPBGT_{i\to j}$ are the margin value and margin step, BR_i and BR_j are the call blocking rates in cells i and j, and β is the diffusion parameter for closed-loop gain control. In (5), it is observed that the change of margins in an adjacency is proportional to the difference in blocking rate between neighbor cells. Hence, equilibrium will not be reached until this difference is negligible. The value of β controls the speed of convergence to equilibrium and the absence of oscillations around the stable point. For symmetry reasons, changes in both directions of the adjacency have the same magnitude but opposite signs. Thus, the initial degree of hysteresis is maintained throughout the tuning process. In this work, the hysteresis is ensured by fixing

$$HoMarginPBGT_{i\to j}^{(n+1)} + HoMarginPBGT_{j\to i}^{(n+1)} = 2\sigma_{sf}\,, \tag{7}$$

where σ_{sf} is the standard deviation of the slow fading term. Likewise, $HoMarginPBGT_{i\to j} \in [-24, 24]$ dB. This method is hereafter referred to as *Slow HO Margin Control* (SHMC).

3.2. Tuning of Handover Signal-Level Constraints

When SHMC is enabled, signal-level constraints must be tuned to avoid excessive call quality impairment, as HO to a worse cell is permitted. Otherwise, it might happen that, after a HO, the received signal level in the new cell was not enough to compensate for the interference in that cell.

In GERAN, measurement reports comprising signal-level (i.e., RXLEV) and signal-quality (i.e., RXQUAL) measurements for active connections are sent from mobile and base station to the base station controller every 480 ms. These reports can be stored in the NMS and later be used to estimate the overall interference level in any particular cell from the relationship between these two indicators[1]. Since interference levels are not constant in time and space, the relationship between RXLEV and RXQUAL in a cell is not deterministic, but rather probabilistic (i.e., for a certain signal-level value, different signal-quality values are possible, depending on instantaneous interference and propagation conditions). The method described in [18] deals with this uncertainty by treating RXLEV and RXQUAL as random variables. The method first estimates the cumulative density function of RXQUAL conditioned to RXLEV (i.e., the probability of experiencing, at least, a certain signal quality, given that a certain signal level is received) on a per-cell basis. From this information, the minimum RXLEV value that ensures that the outage probability (i.e., probability that signal quality is not acceptable) is below a certain threshold in a cell is computed. More formally, this minimum value, $RxLev_{min}$, is defined as

$$RxLev_{min} = \min\{\, x \mid P(\text{RXQUAL} > RxQual_{min} \mid \text{RXLEV} = x) \leq \alpha\} \tag{8}$$

(i.e., minimum RXLEV that ensures that the probability of RXQUAL being worse than $RxQual_{min}$ is less than α), where $RxQual_{min}$ and α are internal parameters defining the minimum acceptable signal quality and the target outage probability, respectively. Figure 1 illustrates an example of the process. The surface in the figure represents the probability of experiencing a signal quality better than $RxQual$ when a signal level $RxLev$ is received in a cell. In the example, the parameters $RxQual_{min}$ and α have been set to 4 and 0.5, respectively. These parameters define a vertical and a horizontal plane, respectively, whose intersection with the surface is the required minimum signal level, $RxLev_{min}$. In the example, $RxLev_{min}$=-104dBm. Generally speaking, highly-interfered cells show large values of $RxLev_{min}$, while non-interfered cells show values of $RxLev_{min}$ close to receiver sensitivity.

In this work, $RxQual_{min}$ is fixed to 4 and 5 for non-hopping and hopping transceivers, respectively, to provide similar Frame Error Rates (FER) values after the decoding process [21]. However, the best value of α must still be decided. A restrictive value might lead to excessive signal-level constraints, reducing the number of cells in the HO candidate list. In these conditions, both the macro-diversity and trunking gain would be unnecessarily reduced. On the other hand, a loose value proves ineffective to avoid HO to a bad cell. This issue is solved by the method discussed next. The above-described method is referred to as *Optimization of Signal-Level Constraints* (OSLC).

[1] In this context, overall means average in users, time and space.

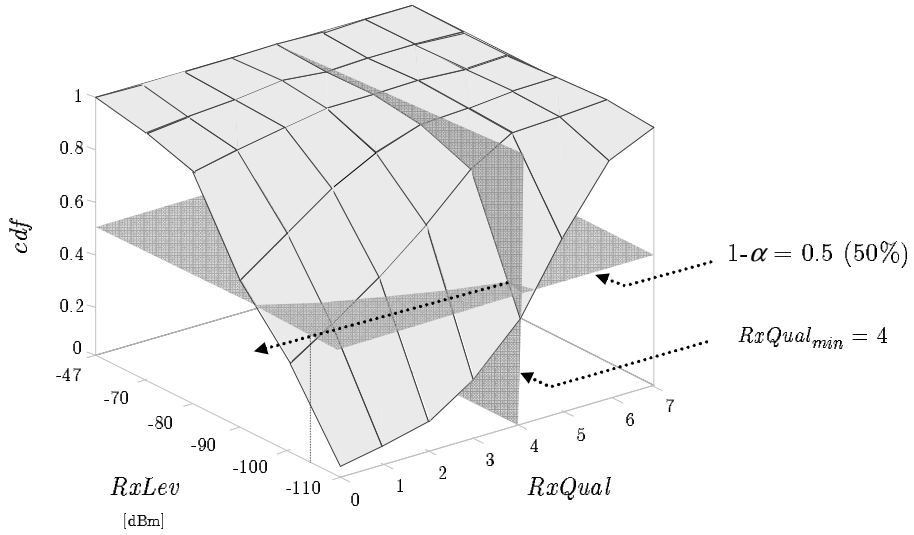

Figure 1. An example of $cdf_{RxQual/RxLev}$ surface.

3.3. Fuzzy Tuning of Handover Margins and Signal-Level Constraints

The following method solves some of the issues of previous algorithms, which are summarized as follows:

1) In SHMC, the margin increment only depends on the blocking difference in the adjacency, regardless of the current value of the margin. However, experience has shown that sensitivity to changes is greatly increased when margins become negative. Thus, it is advantageous to reduce the magnitude of changes once margins become negative. This can be achieved by adjusting the diffusion parameter, β, which can be interpreted as a gain-scheduling mechanism.

2) In OSLC, signal-level constraints are adjusted based on interference statistics in the target cell. Thus, all adjacencies with the same target cell have the same value of signal-level constraint. Alternatively, the target outage probability in OSLC, α, can be adjusted on an adjacency basis based on the current state of margins. Thus, $\alpha_{i\rightarrow j}$ (and, hence, $RxLevMinCell_{i\rightarrow j}$) should be restricted only when $HoMarginPBGT_{i\rightarrow j} < 0$. By adapting $\alpha_{i\rightarrow j}$ instead of $RxLevMinCell_{i\rightarrow j}$, the overall interference in the target cell can still be taken into account by OSLC.

3) In SHMC, only blocking criteria have been taken into account to compute the margin increment. However, interference issues should also be taken into account in those adjacencies where source and target cell share frequencies. Although this situation is avoided in the Broadcast Control CHannel (BCCH) transceiver by careful planning, it is not the case for the rest of transceivers, where tight frequency reuses are normally used. This is not an issue if HO margins are positive. From (2), it can be deduced that the PBGT value gives an estimation of the Carrier-to-Interference Ratio (CIR) after HO if frequency collision occurs between source and target cell. Thus, positive margin settings ensure positive CIR values after HO. However, this is not the case for negative margin values. In this case, it might happen that a mobile station sent to a neighbor cell experienced bad call quality due to interference from the old (i.e.,

strongest) cell, even if the overall interference level in the new cell is low (hence, note that OSLC does not solve this problem). To avoid this situation, tuning is restricted to neighbors sharing frequencies with the original cell by setting the minimum PBGT HO margin on a per-adjacency basis. More specifically, it is ensured that

$$HoMarginPBGT_{i\to j} \geq CIR_{min} + 10\log p_{c_{i\to j}} \ , \tag{9}$$

where CIR_{min} is the target CIR value (i.e., 9dB in this work) and $p_{c_{i\to j}}$ is the interfering collision probability between source and target cell, defined as [22]

$$p_{c_{i\to j}} = \begin{cases} 0 & \text{if } N_{f_{i,j}} = 0, \\ \frac{a_f}{N_{f_{i,j}}} \frac{A_{c_i}}{N_{ts_i}} & \text{if } N_{f_{i,j}} > 0, \end{cases} \tag{10}$$

where a_f is the service activity factor, $N_{f_{i,j}}$ is the number of frequencies shared by cells i and j, A_{ci} is the average carried traffic in the serving cell and N_{tsi} is the number of time slots for traffic purposes in the serving cell. For a non-hopping transceiver, $N_{f_{i,j}}$ is 0 for non-interfered cells and 1 for interfered cells. For a hopping transceiver, $N_{f_{i,j}}$ is the number of frequencies in the frequency hopping list. In case of several transceivers in the neighbor cell, a weighted sum can be used to account for the different collision probability across transceivers. Generally speaking, in adjacencies where source and target cell share frequencies and source cell is highly loaded, margins are restricted to be positive, regardless of the actual overall interference level in the target cell.

4) In SHMC, equilibrium is reached when blocking is the same in adjacent cells. To achieve this goal in the most efficient way, two refinements slightly favor those adjacencies with a lower impact on network quality when re-allocating traffic. First, the interfering collision probability is used to compute the margin increment in SHMC and the target outage probability for OSLC. Thus, interfering neighbors are penalized. Second, a slow-return mechanism to the default configuration (i.e., positive margin values) is implemented to favor adjacencies with positive margins at the expense of the ones with negative margins. Thus, cells continue to re-shape after equalizing blocking, searching for a better balance among all neighbor cells.

To ease development, the method is designed as a fuzzy controller [23]. Fuzzy inference systems are especially suitable for algorithms described in linguistic terms. As shown in Figure 2, the controller consists of two modules: one devoted to the optimization of margins and the other to signal-level constraints. The module in Figure 2.a. computes the margin increment, $\delta HoMarginPBGT_{i\to j}$, from the blocking rate difference, the current margin value and the interfering collision probability in the adjacency. The module in Figure 2.b. computes the target outage probability, $\alpha_{i\to j}$, from the same indicators. Then, the value of $\alpha_{i\to j}$ is used in OSLC to compute $RxLevMinCell_{i\to j}$ from statistics in cell j.

For simplicity, both modules are designed based on the Takagi-Sugeno approach [24]. Each module consists of three stages: fuzzification, inference and defuzzification. In the *fuzzification* stage, each (crisp) value of the input variables is mapped into a set of fuzzy (or linguistic) variables. This mapping is made by a membership function, $\mu_{mn}(x_m)$, which defines the degree with which each value of the input variable m, x_m, is associated to

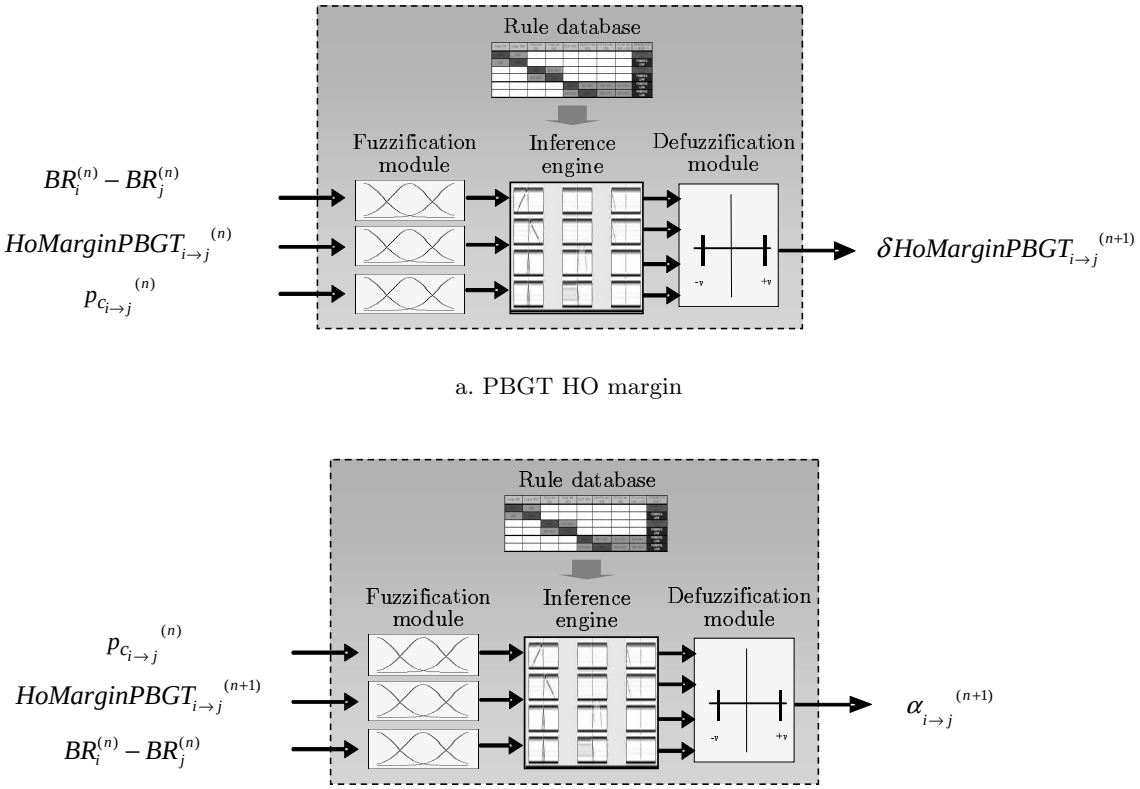

a. PBGT HO margin

b. Target outage probability

Figure 2. Structure of the fuzzy controller.

the fuzzy variable n. Figure 3 depicts the membership functions used in the method. As observed in the figure, each input and output is classified in terms of linguistic variables, ranging from extremely low (EL) to extremely high (EH). In selecting the number of these variables, a trade-off has been made between precision and complexity. The number of input membership functions is large enough to classify the state of adjacencies as precisely as an operator would do, while keeping the number of states small to reduce the effort of defining the set of control rules. Likewise, the number of output membership functions is large to allow fine parameter control. For simplicity, the selected input membership functions are trapezoidal, triangular or constant. The overlap between input membership functions is the key to crisp input values being associated to several linguistic variables simultaneously. In contrast, the output membership functions are constant functions. In the *inference* stage, a set of 'if-then' rules defines the mapping of the input to the output in linguistic terms. Unlike classical expert systems, where only one rule is fired at a time, several rules can be fired simultaneously in a fuzzy system depending on the degree in which their antecedents are satisfied. Table I summarizes the set of rules that describe the tuning process. For instance, rule 1 reads as: "if blocking difference is very large and the current margin is very large, then the HO margin step is extremely large". Briefly, the margin increment, $\delta HoMarginPBGT_{i\to j}$, and the target outage probability, $\alpha_{i\to j}$, are larger for adjacencies that display large blocking difference between source and target cell, cells do not share frequencies and current margin values are positive. To maintain

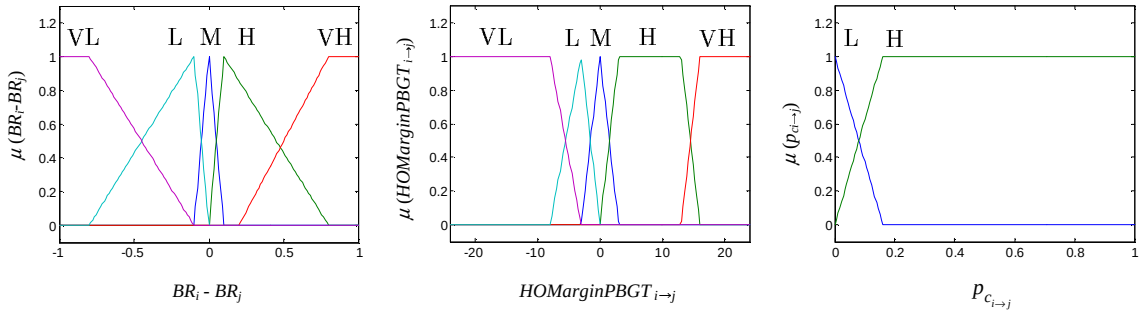

a. Inputs

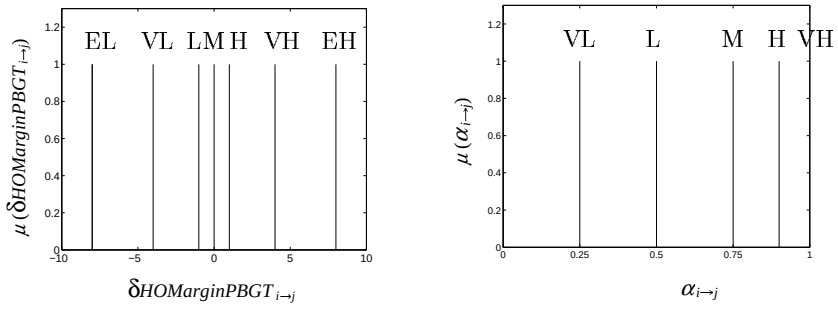

b. Outputs

EL: Extremely Low, VL: Very Low, L: Low, M: Medium, H: High, VH: Very High, EH: Extremely High

Figure 3. Membership functions in the fuzzy controller.

hysteresis, only one direction of the adjacency is directly optimized by the controller (i.e., the one with $BR_i - BR_j > 0$). This justifies that $BR_i - BR_j$ can only be medium (M), high (H) or very high (VH). In the *defuzzification* stage, the output value is obtained from the aggregation of all rules, for which the center-of-gravity method [23] is adopted.

An example is given to illustrate how the algorithm works. Let (i,j) be an adjacency at the beginning of the tuning process, where i is overloaded, j is underutilized and both share a reduced number of frequencies. More specifically, $BR_i - BR_j = 1$, $p_{ci\to j} = 0.17$ and $HoMarginPBGT_{i\to j} = 8$dB. From Figure 3.a., $BR_i - BR_j$ is VH, $HoMarginPBGT_{i\to j}$ is H and $p_{ci\to j}$ is H. From Table I, it is deduced that only rules 3 and 13 are fired, resulting in $\delta HoMarginPBGT_{i\to j}$ is VL and $\alpha_{i\to j}$ is VH. In Figure 3.b., it is observed that these values correspond to $\delta HoMarginPBGT_{i\to j} = -4$dB and $\alpha_{i\to j}$=0.99 (i.e., large decrement in margin and loose significance in OSLC). This results in $HoMarginPBGT_{i\to j} = 4$ dB and $RxLevMinCell_{i\to j} = -110$dBm.

The above-described method is referred to as *Fuzzy Slow HO Margin Control-Fuzzy Optimization of Signal-Level Constraints* (FSHMC+FOSLC).

3.4. Tuning of Cell (Re)Selection Offsets

The previous method solves congestion in a cell by modifying the service area of neighbor cells. As a result, many users are sent to a cell other than the best serving cell in the early stages of the call connection. This leads to an increase of the number of HOs in the network, which can be significant in a low-mobility environment. To keep this increase as

Table I. Set of fuzzy control rules.

Rule no.	$BR_i - BR_j$	$HoMarginPBGT_{i\to j}$	$p_{c_{i\to j}}$	$\delta HoMarginPBGT_{i\to j}$
1	VH	VH	-	EL
2	VH	H	L	EL
3	VH	H	H	VL
4	VH	M|L|VL	L	VL
5	VH	M|L|VL	H	VL
6	H	$\overline{\text{M\|L\|VL}}$	L	VL
7	H	$\overline{\text{M\|L\|VL}}$	H	L
8	H	M|L|VL	L	L
9	H	M|L|VL	H	L
10	M	VH	-	L
11	M	H	-	M
12	M	M|L|VL	-	H
Rule no.	$BR_i - BR_j$	$HoMarginPBGT_{i\to j}$	$p_{c_{i\to j}}$	$\alpha_{i\to j}$
13	-	M|H|VH	-	VH
14	VH	L	L	H
15	$\overline{\text{VH}}$	L	L	M
16	$\overline{\text{M}}$	L	H	M
17	M	L	H	L
18	-	VL	-	VL

| : Logical OR, $\overline{(\bullet)}$: Logical NOT

small as possible, CRS offsets can be adjusted to synchronize the dominance area of cells in CRS to the one defined by HO. Cells with positive (negative) HO margins in outgoing adjacencies should have a positive (negative) bias, as their service area defined by HO is larger (smaller). Unfortunately, CRS offsets are defined on a cell basis, whereas HO margins are defined on an adjacency basis. Hence, a single offset value must be calculated by averaging margins in all adjacencies of a cell. In this work, a weighted average is used to give priority to those adjacencies that tend to attract most HOs from/to a cell. Thus, the value of *CellReselectOffset* in a cell is calculated as

$$CellReselectOffset_i^{(n+1)} = \max\left(0, -\frac{\sum\limits_{j\in N(i)} \Delta HoMarginPBGT_{i\to j}^{(n+1)} \left(N_{hoi\to j}^{(n)} + N_{hoj\to i}^{(n)}\right)}{\sum\limits_{j\in N(i)} \left(N_{hoi\to j}^{(n)} + N_{hoj\to i}^{(n)}\right)}\right), \tag{11}$$

where $N(i)$ is the set of neighbors of cell i, $\Delta HoMarginPBGT_{i\to j}$ is the margin displacement from the default settings, and $N_{hoi\to j}$ and $N_{hoj\to i}$ are the number of HOs in each direction of the adjacency. Basically, a cell with $\Delta HoMarginPBGT_{i\to j} < 0\ \forall j$ (i.e., reduced HO dominance area) leads to $CellReselectOffset_i > 0$ (i.e., negative bias). Conversely, a cell with $HoMarginPBGT_{i\to j} > 0\ \forall j$ would lead to $CellReselectOffset_i < 0$, which is truncated to 0. This method is referred to as *Adaptation of Cell Re-selection Offsets* (ACRO).

4. Simulations

In the absence of a precise analytical model that predicts the impact of the optimized parameters on interference levels, performance assessment is based on system-level simulations. For clarity, the simulation environment and the assessment methodology are outlined first and simulation results are subsequently discussed.

4.1. Simulation Setup

Simulations are performed on a dynamic system-level GERAN simulator. Table II shows the default values of the main simulation parameters. The simulation scenario intends to model a macro-cellular urban environment with severe congestion problems to push the proposed methods to their limits. The layout, depicted in Figure 4.a., consists of 108 cells in 36 tri-sectorized sites uniformly distributed. For computational efficiency, a single transceiver is simulated per cell. This transceiver can model either a Traffic-CHannel (TCH) or the BCCH transceiver, depending on features in use. Several frequency reuse schemes are simulated, including random hopping (RH) and non-hopping (nH) cases. The number of frequencies in the scenario is 9 and 12 for TCH and BCCH transceivers, respectively. The default frequency reuse scheme is TCH 1/3 RH3 (details about reuse schemes can be found in [2]). Only the downlink is simulated, as it is the most restrictive link in GERAN [21]. Likewise, only circuit-switched voice traffic is generated, as it is the main service affected by the tuning process. To reproduce a realistic case, traffic demand is unevenly distributed in the scenario following a log-normal distribution [5], implemented as in [25]. Figure 4.b. shows the probability of starting a call in a location. It is observed that the spatial traffic distribution has a central peak, which justifies the need for traffic sharing. This can be considered as a worst-case scenario, since most of the traffic is generated in a few cells, which are adjacent to each other. As a result, limited trunking gain is achieved by traffic sharing. The average traffic load is set to 36%, which would result in a low blocking probability (i.e., 0.007) if traffic was evenly distributed. Hence, it is the imperfect spatial match between traffic demand and deployed resources (and not the overall lack of resources) what causes congestion.

Six congestion-relief methods are simulated. The first two are classical RRM features. Directed Retry (DR) [8] is used as a benchmark, as it is the default method used to cope with congestion problems. Thus, other methods are added on top of DR, since DR is hardly ever disabled by operators. In DR, blocked calls are assigned to cells other than the serving cell. For a cell to be a potential target, the received signal level must be above a certain threshold, defined by the *DrThreshold* parameter. In this work, the latter is set to its maximum value (i.e., -47dBm) for neighbor cells that are co-channel interferers of the source cell. Thus, parameters in other adjacencies can be adjusted in a wider range and more freedom is given to other traffic sharing methods, as more room for quality impairment is available. For a similar reason, conservative settings are set for DR when combined with other techniques (i.e., *DrThreshold*=-95dBm). The second method is the diffusive load-sharing algorithm known as Traffic-Reason HO (TRHO) [10]. In this feature, PBGT HO margins are temporarily reduced when a cell becomes congested. The temporary margin value is defined by the parameter *TrHoMarginPBGT*. To avoid instabilities, the load of a neighbor cell must be below a certain limit to be considered as a HO candidate. The other four methods are combinations of the tuning methods described in Section 3: the slow HO margin control (SHMC), the previous method with adaptation of signal-level constraints based only on the interference in the target cell (SHMC+OSLC), the fuzzy

Table II. Simulation parameter settings.

Scenario	TU3, MACRO, cell radius 0.5 km
Propagation model	Okumura-Hata with wrap-around
	Correlated log-normal slow fading, $\sigma_{sf} = 8$ dB
Mobility model	Random direction, constant speed 3km/h
Service model	CS-Voice, mean call duration 80s, activity factor 0.5
Base station model	Tri-sectorized antenna, $EIRP_{max}$=43 dBm
Adjacency plan	Symmetrical adjacencies, 32 per cell
RRM features	Random FH, POC, DTX, DR
HO parameter settings	Qual HO threshold RXQUAL = 4
	PBGT HO margin [-24, 24] dB
	RxLevMinCell [0, 63]
	DrThreshold 15
Average traffic load	36%
Time resolution	SACCH frame (480 ms)
Simulated network time	28 h (per optimization epoch)

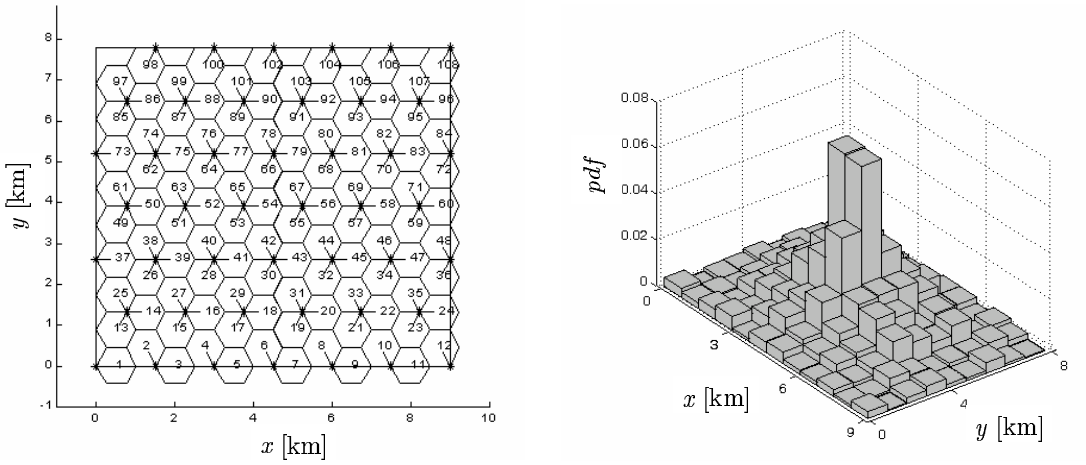

a. Layout b. 2-D spatial traffic distribution

Figure 4. Simulation scenario.

variant that jointly optimizes HO margins and signal-level constraints (FSHMC+FOSLC), and the previous method with adaptation of CRS offsets (FSHMC+FOSLC+ACRO). In self-tuning methods, several optimization steps (referred to as epochs) are performed to emulate the feedback loop of the tuning process. Each epoch comprises 100000 simulation steps, equivalent to 28 hours of actual network time. After each epoch, new parameters are configured in the simulator based on performance indicators of the previous period. Within each epoch, simulation parameters remain unchanged. The speed of the tuning process is controlled by the diffusion parameter, β. For clarity, the value of β will be

specified hereafter by the maximum margin step per epoch, δ. Unless stated otherwise, $\delta = 2$ dB.

4.2. Performance Assessment Methodology

The main performance indicators are the *overall blocking rate*, $\overline{BR}$, and the *overall outage rate*, $\overline{OR}$, defined as

$$\overline{BR} = \frac{N_{bT}}{N_{oT}}\,, \qquad \overline{OR} = \frac{N_{mrT}|_{FER \geq FER_{max}}}{N_{mrT}}\,, \tag{12}$$

where N_{oT} and N_{bT} are the total number of offered and blocked call attempts after DR, respectively, and N_{mrT} and $N_{mrT}|_{FER \geq FER_{max}}$ are the raw number of measurement reports and bad quality reports, respectively. In this work, FER_{max}=5.4%.

The value of a particular network configuration is given by its *penalty*, p, defined as

$$p = \omega_{BR}\left(\frac{\overline{BR}}{\overline{BR}_t}\right)^e + \omega_{OR}\left(\frac{\overline{OR}}{\overline{OR}_t}\right)^e\,, \tag{13}$$

where $\overline{BR}$ and $\overline{OR}$ are the performance figures of the configuration, $\overline{BR}_t$ and $\overline{OR}_t$ are performance target values, e is a constant to penalize the non-fulfillment of objectives, and ω_{br} and ω_{or} are the relative weights of the capacity and quality criteria. Hereafter, $\overline{BR}_t = 0.05$, $\overline{OR}_t = 0.01$, $e = 3$ and $\omega_{br} = \omega_{or} = 1/2$. The former two values are aligned to current operator demands, while the latter two reflect that both targets are equally important. With these settings, a network configuration with $\overline{BR}$=0.05 and $\overline{OR}$=0.01 has p=1.

The value of a method is given by the trade-off between $\overline{OR}$ and $\overline{BR}$ in all network configurations obtained by the method. In self-tuning methods, such configurations are given by the series of configurations reached as tuning progresses, which is referred to as a *trajectory*. For RRM methods, different network configurations can only be obtained by adjusting internal parameters. In particular, the values of *DrThreshold* in DR and *TrHoMarginPBGT* in TRHO are modified to investigate the $\overline{OR}$-$\overline{BR}$ trade-off in these methods. In the absence of an automatic method to tune these parameters, a trial-and-error approach has been followed to select the parameter range to be evaluated.

In principle, the main focus of the analysis is on the asymptotic behavior. However, as self-tuning algorithms gradually change parameters in the real network, not only the steady state but also the transient response is important. To evaluate transient responses, an infinite-horizon discounted model [26] is considered. In this model, the *overall penalty* of a trajectory, P, is calculated as

$$P = (1-\gamma)\sum_{n=0}^{\infty}\gamma^n p_n\,, \tag{14}$$

(i.e., the weighted average of penalties across epochs, p_n). This model takes into account long-term penalties, but future penalties are given less importance according to a geometric law with discount factor γ, where $0 \leq \gamma \leq 1$. The latter formula reflects that, in live environments, early rewards are preferred to delayed rewards, since traffic conditions might greatly vary with time and situations of persistent congestion are solved in the long-term by other approaches. To reduce the simulation effort, it is assumed that equilibrium is reached after h epochs. Thus, the overall penalty is calculated as

$$P \approx (1-\gamma)\sum_{n=0}^{h-1}\gamma^n p_n + \sum_{n=h}^{\infty}\gamma^n p_h = (1-\gamma)\sum_{n=0}^{h-1}\gamma^n p_n + \gamma^h p_h \,, \tag{15}$$

where p_h is the penalty in the last simulated epoch. Hereafter, h=19 and γ=0.85. A horizon of 19 epochs means that only 20 epochs are simulated (i.e., 1 initial state + 19 tuning steps). This horizon should be large enough to ensure that the system has reached equilibrium. Even if this is not the case, the low value of γ ensures that the influence of epochs beyond this point is negligible. For RRM methods, the performance is the same across epochs, as internal settings do not change from epoch to epoch. Hence, each internal setting has its own value of P. From (15), it can be easily deduced that P=p for these methods, where p is the penalty in any one epoch.

To estimate the increase in signaling load due to an increased number of HOs, the *overall HO rate*, $\overline{HR}$, is evaluated as

$$\overline{HR} = \frac{N_{hoT}}{N_{cT}} \,, \tag{16}$$

where N_{hoT} and N_{cT} are the raw number of HOs and carried calls, respectively.

4.3. Simulation Results

The first experiment shows the limitations of classical approaches over a test case. Figure 5 shows the performance of several methods in the scenario with reuse TCH 1/3 RH3. In DR and DR+TRHO, each point represents a different configuration of internal parameters. In DR, from left to right, each point corresponds to a value of *DrThreshold* in the set {-95, -97, -99, -101, -103} dBm. In DR+TRHO, each point corresponds to a value of *TrHoMarginPBGT* in the set {0, -4, -8} dB. In contrast, points in the DR+SHMC curve represent the different network parameter configurations as reached by the tuning process (i.e., the initial situation on the upper-left and equilibrium inside the cloud of points on the lower-right). In the figure, it is observed that all methods reduce $\overline{BR}$ by increasing $\overline{OR}$. Despite its simplicity, DR is an effective method to solve localized congestion problems when *DrThreshold* is adjusted. In particular, $\overline{BR}$ can be decreased from 10.8% to 3.9% (i.e., almost 3-fold reduction) when changing *DrThreshold* from -95 to -103dBm. However, this is achieved at the expense of a significant impairment of the overall connection quality, which is evident from the increase of $\overline{OR}$ from 0.6% to 2.7% (i.e., 5-fold increase). In contrast, DR+TRHO is totally ineffective. Even if the addition of TRHO leads to a slight reduction in $\overline{BR}$, no further benefit is obtained by tuning *TrHoMarginPBGT*. This result is caused by the mechanism that prevents users from being sent to cells with high loads. Since most congested cells in the scenario are adjacent to each other, no traffic sharing is triggered among these cells. Finally, it is observed that DR+SHMC performs reasonably well in the initial epochs (upper-left), when HO margins are still positive in all adjacencies. Thus, $\overline{BR}$ is reduced from 10.8% to 9.4% with no quality impairment. However, once margins become negative (knee of the curve), severe call quality impairment is observed, while limited blocking relief is attained. From this result, it can be concluded that, with the classical method to tune PBGT HO margins, there is no point in setting negative values.

The next experiment highlights the cause of limitations by testing the previous methods with different frequency reuse schemes. Figures 6.a.-b. show $\overline{BR}$ and $\overline{OR}$ in equilibrium for 4 methods with 5 reuse schemes. The analysis is first focused on DR. From the first two sets of bars in Figure 6.a., it can be deduced that $\overline{BR}$ is halved when DR is enabled

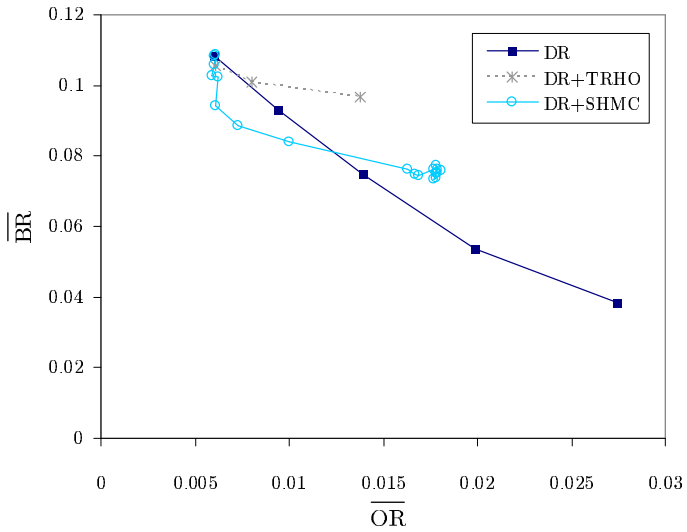

Figure 5. Performance of classical congestion-relief methods in the scenario.

(note the logarithmic scale). However, Figure 6.b. shows that unrestricted DR can severely deteriorate $\overline{OR}$, regardless of the conservative value of *DrThreshold*. When a call is redirected to a cell other than its original cell, it might experience bad quality due to proximity to an interferer. This situation is rather common in TCH 1/1 RH9, as source and target cell in DR always share the same frequencies. For the latter scheme, $\overline{OR}$ increases from 0.1% to 2.5% when DR is enabled with no restrictions. It is thus clear that restricting DR to neighbors potentially interfered by the original cell can improve network quality. With this approach, $\overline{OR}$ in TCH 1/1 RH9 can be reduced by one order of magnitude, but at the expense of loosing most of the traffic sharing capability of DR. Such a loss is negligible for loose frequency reuses, where the number of co-channel interferers in the neighbor-cell list is small. These results prove the benefit from restricting DR to interfered neighbors. Note that the higher $\overline{BR}$ for the BCCH transceiver under the same traffic is due to the use of 6 time slots instead of 8, which reflects the existence of signaling channels on this transceiver. Likewise, the higher $\overline{OR}$ in the BCCH transceiver is due to the lack of features such as DTX, POC and FH. The effect of SHMC can be isolated from that of DR by comparing the last two sets of bars. It is observed that SHMC can reduce blocking at the expense of a non-negligible quality impairment. As in other methods, the impairment from SHMC is more severe in tighter frequency reuses. For instance, $\overline{OR}$ increases by two orders of magnitude when SHMC is enabled in TCH 1/1 RH9. These results provide strong evidence that most traffic sharing techniques experience interference problems in tight frequency reuses, unless countermeasures are adopted. The rest of the analysis is restricted to the TCH 1/3 RH3 scheme, although similar results are expected with other frequency reuses. Likewise, restricted DR is always used.

The next experiment shows how interference problems in SHMC can be alleviated by tuning HO signal-level constraints. For this purpose, SHMC is tested with different values of *RxLevMinCell*. Figure 7 shows the performance of SHMC with *RxLevMinCell* set to {-105, -100, -95} dBm in all adjacencies in the scenario. It is observed that, in the initial stage of the tuning process (i.e., upper-left), the higher (i.e., the more restrictive) *RxLevMinCell*, the higher $\overline{OR}$ (i.e., the lower overall network quality). In particular, in the first epoch, where margins have not changed yet, $\overline{OR}$ increases from 0.6% to 0.75% by

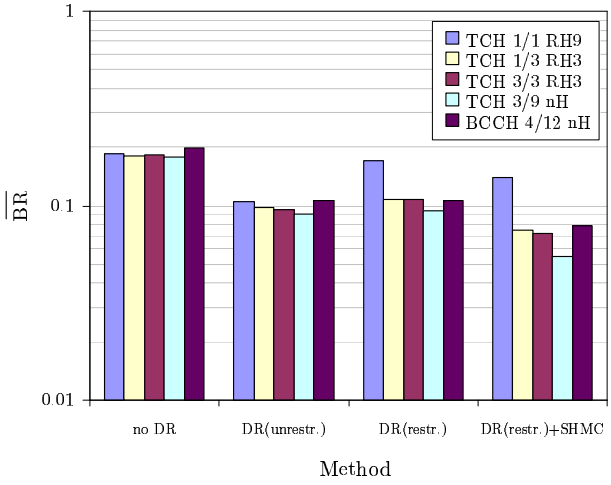

a. Blocking rate

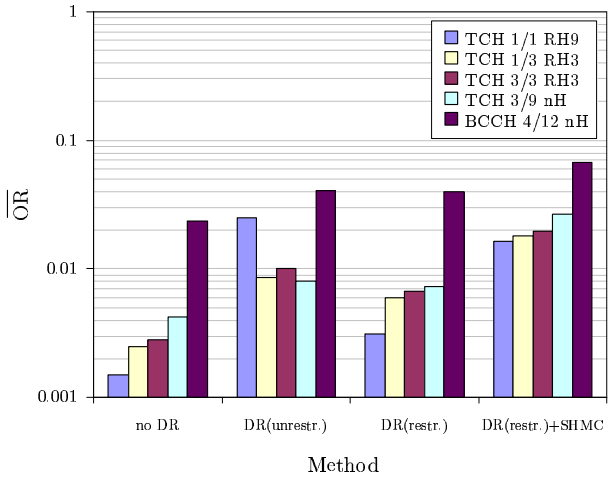

b. Outage rate

TCH: Traffic CHannel, BCCH: BroadCast CHannel, RH: Random Hopping, nH: non-Hopping

Figure 6. Influence of frequency reuse scheme on the performance of classical methods.

raising *RxLevMinCell* from -105dBm to -95dBm. This is mainly due to the fact that, when positive margin values are used, PBGT HO ensures that a mobile station is never sent to a worse cell. Hence, increasing HO constraints only leads to rejection of valid candidate neighbors, which might be used in the case of severe shadowing of the serving cell. In these conditions, unnecessary restriction of HO through tight signal-level requirements contributes to worsen (rather than enhance) network quality. On the contrary, when HO margins become negative (i.e., lower-right), restricting HO can prevent quality problems. For instance, $\overline{OR}$ in equilibrium can be reduced from 1.8% to 1.0% (i.e., almost halved) with a negligible increase in $\overline{BR}$ by increasing *RxLevMinCell* from -105dBm to -95dBm. From these results, it can be concluded that signal-level constraints must adapt to the current state of HO margins.

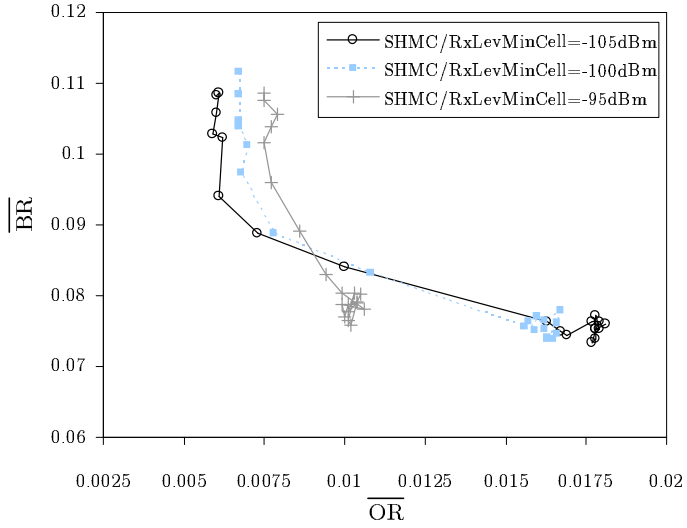

Figure 7. Influence of signal-level constraints on the performance of SHMC.

The following experiment shows the benefit of restricting HO to cells that are more interfered when using SHMC. Figure 8 presents the results of using SHMC and OSLC simultaneously but independently. In SHMC+OSLC, *RxLevMinCell* is optimized on a per-adjacency basis by applying OSLC over statistics in the target cell of each adjacency. The results of SHMC with homogeneous *RxLevMinCell* settings are superimposed for comparison purposes. For a fair comparison, it is important to ensure that SHMC+OSLC ends up with a similar level of restriction, i.e., even if *RxLevMinCell* is modified on an adjacency basis, the average value of *RxLevMinCell* in the scenario should be maintained. This was achieved by setting α=0.5 in OSLC. After the initial epoch, where *RxLevMinCell*=-105dBm, OSLC modifies *RxLevMinCell* in the adjacencies, averaging -98dBm in the scenario. This value can be inferred from the figure, as the SHMC+OSLC curve is quite close to that of SHMC with *RxLevMinCell*=-100 dBm. After some loss of quality in the initial epochs, the quality improvement is noticeable in the last epochs, when HO margins become negative. Concretely, $\overline{OR}$ in equilibrium can be reduced from 1.8% to 1.3% when OSLC is introduced. It is worth noting that this quality improvement is achieved without increasing $\overline{BR}$. From these results, it is clear that optimizing *RxLevMinCell* on an adjacency basis can lead to a better trade-off between network quality and capacity in SHMC.

The following experiment proves the benefit of jointly optimizing *HoMarginPBGT* and *RxLevMinCell* by the fuzzy controller proposed. Figure 9 presents the results of FSHMC+FOSLC together with the best approaches described so far. From the figure, it is clear that FSHMC+FOSLC performs extremely well throughout the whole trajectory. In equilibrium, FSHMC+FOSLC provides the lowest $\overline{OR}$ (i.e., 0.9%) with only 0.7% absolute more $\overline{BR}$ than the best solution achieved by other tuning methods. More important, for any epoch, there is no feasible solution that would enhance $\overline{BR}$ without impairing $\overline{OR}$ (i.e., the FSHMC+FOSLC solution is always non-dominated). Thus, it is expected that the FSHMC+FOSLC curve provides an accurate estimation of the Pareto-front for the tuning of HO margins. This result is just a consequence of the gradual increase of HO signal-level constraints as HO margins decrease.

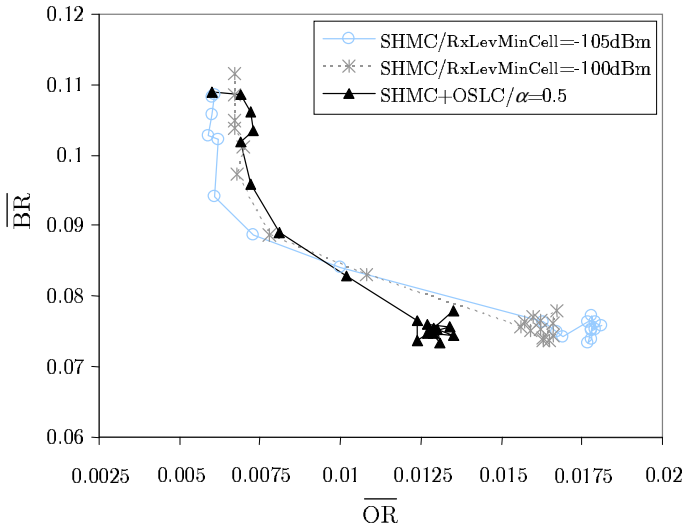

Figure 8. Performance of the combination of SHMC and OSLC.

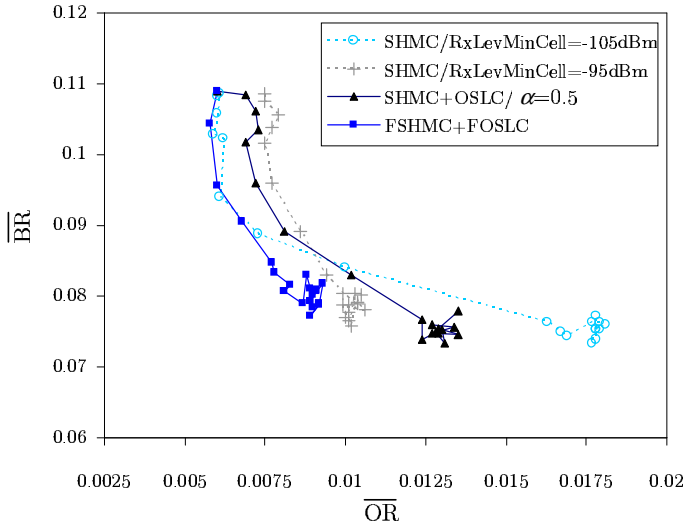

Figure 9. Performance of the combination of FSHMC and FOSLC.

The analysis now focuses on penalty figures. Table III presents the performance of different methods in terms of the overall penalty, P, the minimum penalty of an epoch in the trajectory, p_{min}, and the penalty in the equilibrium state, p_{eq}. Obviously, all three indicators coincide for RRM methods, as the trajectory consists of a single solution. At first glance, it is observed that no method achieves the performance targets in the scenario, as none of them shows a value of P below 1. This result shows conclusively that the test case is pushing the methods to their limits. It is also clear that the default network configuration, where only DR is enabled, has a large penalty due to the large blocking in the scenario. TRHO has slightly less penalty. From the values in the first column, it might be tempting to conclude that some self-tuning methods do not perform better than RRM methods. However, comparison based on P is biased, since this figure in RRM

Table III. Penalty of methods in the scenario.

Type	Method	P	p_{min}	p_{eq}
RRM	DR, *DrThreshold*=-95dBm (default)	2.52	2.52	2.52
	TRHO, *TrHoMarginPBGT*=0 dB	2.42	2.42	2.42
Self-tuning	SHMC, *RxLevMinCell*=-105dBm, δ=8 dB	2.52	2.24	2.68
	SHMC+OSLC, α=0.5, δ=8 dB	2.12	1.88	1.99
	FSHMC+FOSLC	1.95	1.59	1.67

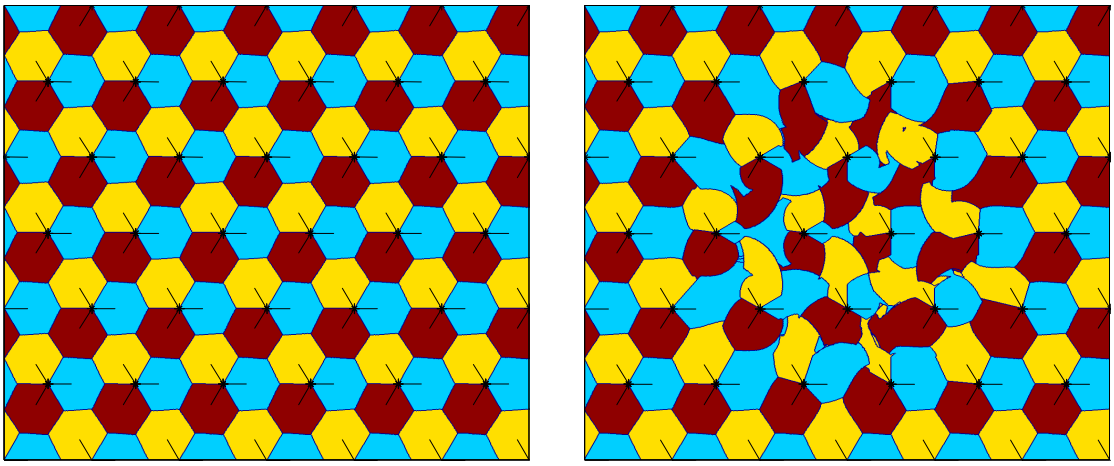

a. Before tuning b. After 20 epochs

Figure 10. Dominance areas defined by the handover process.

methods would only reflect the performance of one state and not the aggregation of the whole trajectory to reach that state from scratch. In contrast, self-tuning methods begin with a network state that is far from optimal, which is progressively improved. For a fair comparison, the assessment must be based on either the best or the last epoch (i.e., p_{min} or p_{eq}, respectively). Based on p_{min}, the performance of self-tuning methods is above that of TRHO and DR only. FSHMC+FOSLC proves to be the best method based on all criteria. Concretely, FSHMC+FOSLC has 37% lower p_{min} than DR only. Table III also shows that the self-tuning methods proposed do not necessarily have the lowest penalty in equilibrium. On the contrary, some methods end up with a penalty that is larger than the one at the origin (i.e., $p_{eq} > p_{min}$). This is due the fact that the proposed methods aim at balancing blocking between adjacent cells, without checking p during the tuning process. Thus, even if p is initially reduced due to blocking relief, the subsequent loss of network quality causes that, at some epoch, p starts to increase again. From the table, it is clear that FSHMC+FOSLC shows the smallest difference between p_{eq} and p_{min}.

The following analysis quantifies the impact of self-tuning on network signaling load. While $\overline{HR}$ is 0.32 with DR only, $\overline{HR}$ in SHMC is 1.91 (i.e., 6 times higher). Tuning signal-level constraints by SHMC+OSLC reduces $\overline{HR}$ down to 1.58. The additional rules in FSHMC+FOSLC help to reduce $\overline{HR}$ even more, but $\overline{HR}$ in FSHMC+FOSLC is still 1.13 (i.e., 3.5 times that of DR). The reason can be found in the service area of cells after

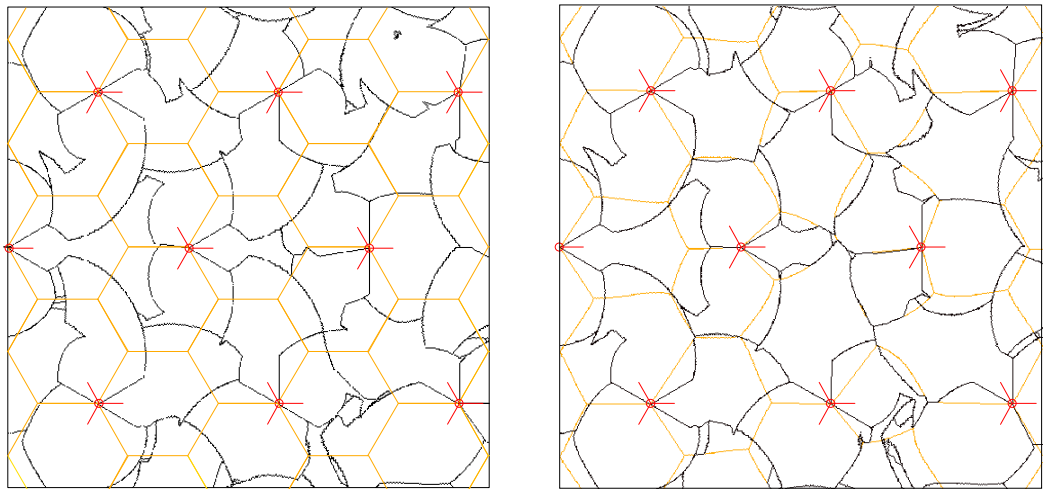

a. No *CellReselectOffset* tuning b. *CellReselectOffset* tuning

Figure 11. Dominance areas defined by the cell re-selection and handover processes.

tuning. Figure 10 illustrates the HO dominance areas before and after tuning. It is observed that cells in the center of the scenario reduce their dominance area, while surrounding cells increase their dominance area. As the dominance area of some cells is significantly reduced, many users accessing these cells are handed over to adjacent cells. Tuning CRS offsets by ACRO reduces $\overline{HR}$ down to 0.67 (i.e., half the one in FSHMC+FOSLC, and only twice that of DR only). The reason can be found in Figure 11, where the final CRS and HO dominance areas are compared. Figure 11.a. and b. show the results without and with ACRO, respectively. For clarity, only a limited area in the center of the scenario is shown. In both figures, the contour of the dominance areas in CRS and HO is shown by an orange and a black line, respectively. From the comparison of both figures, it can be deduced that CRS and HO dominance areas differ less in Figure 11.b., which means that less users will be handed over shortly after the first access.

The last experiment evaluates the increase of network capacity when FSHMC+FOSLC is enabled. The old network capacity is defined as the carried traffic in the default situation (i.e., DR, *DrThreshold*=-95dBm, *RxLevMinCell*=-105dBm). The new network capacity is defined as the maximum carried traffic that ensures that, in the new equilibrium state, $\overline{BR} \leq \overline{BR}_0 = 10.8\%$ and $\overline{OR} \leq \overline{OR}_t = 1\%$ (i.e., blocking is no greater than with the current traffic demand, while still satisfying the minimum overall quality target). In the previous definition, it has been assumed that, from the operator's perspective, there is no extra benefit in enhancing network quality, once the quality target is ensured. To estimate the new capacity, the traffic demand in the scenario is increased gradually, maintaining the spatial distribution, until one of the two conditions is violated. Simulation results show that, after enabling FSHMC+FOSLC, the average carried traffic per cell can increase from 2.56E to 2.95E (i.e., 15% increase), while still maintaining both requirements. It can thus be concluded that FSHMC+FOSLC is an effective method to increase network capacity when traffic demand is unevenly distributed. It is worth noting that other tuning approaches do not provide any capacity increase in these conditions, since $\overline{OR} > \overline{OR}_t$ in equilibrium with the old traffic demand (i.e., the traffic demand should decrease to reach the network quality target).

It is worth noting that, although the analysis is restricted to slow moving users (i.e., 3km/h), similar results are obtained with fast moving users (i.e., 50km/h). Note that the proposed self-tuning method is not an RRM algorithm, but is conceived as a network re-planning procedure based on statistics that are gathered, at most, a few times a day. Since rapid fluctuations (e.g., due to users movement) are filtered out by the statistics collection process, the method can only be used to track trends in the network (i.e., changes in the order of hours or days). Therefore, user speed is not a critical factor when evaluating the speed of tuning and its influence on results can be proved to be small. Finally, it should be pointed out that, although only performance averages have been presented for clarity, confidence intervals for these averages prove to be small due to the large number of simulated steps (and, consequently, calls) per epoch.

5. Conclusions

This paper has investigated the problem of tuning HO margins for traffic sharing in GERAN. Experiments have shown that current approaches suffer from connection quality problems with tight frequency reuses, while also increasing the number of HOs considerably. To solve these problems without reducing congestion relief capabilities, a method has been proposed to jointly optimize HO margins, HO signal-level constraints and CRS offsets. The key to its efficacy is that it restricts HO only when needed, i.e., when HO margins become negative and the target cell is (or could be) highly interfered. In parallel, CRS offsets are tuned to synchronize cell service areas in CRS to the ones in HO. Thus, the number of additional HOs caused by traffic sharing is minimized. Simulation results in an extreme scenario have shown that the proposed method achieves nearly the same blocking rate reduction with half of the outage rate and a three-fold reduction of the number of HOs. More importantly, this technique does not need any hardware upgrade, providing a cost-effective means to increase network capacity. Future work aims to adapt the method proposed here to the HO between different radio access technologies.

References

1. J.Lempiainen and M.Manninen, *Radio Interface System Planning for GSM/GPRS/UMTS*. Kluwer Academic Publishers, 2001.
2. T. Halonen, J. Melero, and J. Romero, *GSM, GPRS and EDGE Performance: Evolution Toward 3G/UMTS*. John Wiley & Sons, 2002.
3. J.Laiho, A.Wacker, and T.Novosad, *Radio Network Planning and Optimisation for UMTS*. John Wiley & Sons, 2002.
4. A. Mishra, *Fundamental of Cellular Network Planning and Optimisation*. John Wiley & Sons, 2004.
5. U.Gotzner, A.Gamst, and R.Rathgeber, "Spatial traffic distribution in cellular networks," in *Proc. 48th IEEE Vehicular Technology Conference*, vol. 2, May 1998, pp. 1994–1998.
6. S.Almeida, J.Queijo, and L.Correia, "Spatial and temporal traffic distribution models for GSM," in *Proc. 50th IEEE Vehicular Technology Conference*, vol. 1, May 1999, pp. 131–135.
7. *3GPP TS 06.02, Half-rate speech; Half-rate speech processing functions; GSM-Phase2+, Release 99*, 3GPP Std., Rev. 8.0.0, Jul 2000.
8. B.Eklund, "Channel utilization and blocking probability in a cellular mobile telephone system with directed retry," *IEEE Transactions on Communications*, vol. 34, no. 4, pp. 329–337, Apr 1986.
9. J.Karlsson and B.Eklund, "A cellular mobile telephone system with load sharing - an enhancement of directed retry," *IEEE Transactions on Communications*, vol. 37, no. 5, pp. 530–535, May 1989.

10. J.Wigard, T.T.Nielsen, P.H.Michaelsen, and P.Morgensen, "On a handover algorithm in a PCS1900/GSM/DCS1800 network," in *Proc. 49th IEEE Vehicular Technology Conference*, vol. 3, Jul 1999, pp. 2510–2514.
11. S.Kourtis and R.Tafazolli, "Adaptive handover boundaries: a proposed scheme for enhanced system performance," in *Proc. 51st IEEE Vehicular Technology Conference*, vol. 3, Jul 2000, pp. 2344–2349.
12. J. Kojima and K. Mizoe, "Radio mobile communication system wherein probability of loss of calls is reduced without a surplus of base station equipment," U.S. Patent 4435840, Mar 1984.
13. D. Lee and C. Xu, "Mechanical antenna downtilt and its impact on system design," in *Proc. 47th IEEE Vehicular Technology Conference*, vol. 2, May 1997, pp. 447–451.
14. N. Papaoulakis, D. Nikitopoulos, and S. Kyriazakos, "Practical radio resource management techniques for increased mobile network performance," in *12th IST Mobile and Wireless Communications Summit*, June 2003.
15. T.Chandra, W.Jeanes, and H.Leung, "Determination of optimal handover boundaries in a cellular network based on traffic distribution analysis of mobile measurement reports," in *Proc. 47th IEEE Vehicular Technology Conference*, vol. 1, May 1997, pp. 305–309.
16. J.Steuer and K.Jobmann, "The use of mobile positioning supported traffic density measurements to assist load balancing methods based on adaptive cell sizing," in *Proc. 13th IEEE Int. Symp. on Personal Indoor and Mobile Radio Communications*, vol. 3, Jul 2002, pp. 339–343.
17. V. Wille, S. Pedraza, M. Toril, R. Ferrer, and J. Escobar, "Trial results from adaptive hand-over boundary modification in GERAN," *Electronics Letters*, vol. 39, no. 4, pp. 405–407, Feb 2003.
18. M. Toril, S. Pedraza, R. Ferrer, and V. Wille, "Optimisation of signal-level thresholds in mobile networks," in *Proc. 55th IEEE Vehicular Technology Conference*, vol. 4, May 2002, pp. 1655–1659.
19. W. Mande, "Evaluation of a proposed handover algorithm for the GSM cellular system," in *Proc. 40th IEEE Vehicular Technology Conference*, May 1990, pp. 264–269.
20. "3GPP TS 45.008, radio subsystem link control," Nov 2001.
21. T. T. Nielsen and J. Wigard, *Performance Enhancements in a Frequency Hopping GSM Network*. Kluwer Academic Publishers, 2000.
22. M. Chiani, E. Agrati, M. Mezzetti, and O. Andrisano, "Frequency and interference diversity in slow frequency hopping multiple access systems," in *Proc. 7th IEEE Personal Indoor and Mobile Radio Communications*, vol. 2, Oct 1996, pp. 648–652.
23. T. Ross, *Fuzzy logic with engineering applications*. McGraw-Hill, 1995.
24. M. S. T. Takagi, "Fuzzy identification of systems and its application to modelling and control," *IEEE Transactions on Systems, Man, and Cybernetics*, vol. SMC-15, pp. 116–132, Jan 1985.
25. B. Ahn, H. Yoon, and J. Cho, "A design of macro-micro CDMA cellular overlays in the existing big urban areas," *IEEE Journal on Selected Areas in Communications*, vol. 19, no. 10, pp. 2094–2104, Oct 2001.
26. L. Kaebling, M. Littman, and A. Moore, "Reinforcement-learning: A survey," *Journal of Artificial Intelligence Research*, vol. 4, pp. 237–285, May 1996.